Available online at www.eccomasproceedia.org
Eccomas Proceedia COMPDYN (2023) 1592-1604

ECCOMAS
Proceedia

COMPDYN 2023
9th ECCOMAS Thematic Conference on
Computational Methods in Structural Dynamics and Earthquake Engineering
M. Papadrakakis, M. Fragiadakis (eds.)
Athens, Greece, 12-14 June 2023

FINITE ELEMENT MODEL FOR RUBBER SEISMIC ISOLATION WITH AND WITHOUT S-SHAPED STEEL DAMPERS

Kai Guo[1,2], **Gaetano Pianese**[1], **Gabriele Milani**[1]

[1] Department of Architecture, Built Environment and Construction Engineering (ABC), Politecnico di Milano
Piazza Leonardo da Vinci 32, 20133 Milano, Italy
e-mail: kai.guo@polimi.it, gaetano.pianese@polimi.it, gebriele.milani@polimi.it

[2] Guangling College of Yangzhou University
Hanjiang South Road 199, 225000 Yangzhou, China
e-mail: 060099@yzu.edu.cn

Abstract

There are novel hybrid base isolation systems proposed to improve the dissipated energy of the base isolation system using different dissipation devices, for instance, shape memory alloy (SMA) wires, ADAS dampers and slit steel dampers. In this paper, a seismic isolator coupled with S-shaped steel dampers (SSSDs) called novel hybrid seismic isolation system, is proposed and investigated. The mechanical property is improved and the displacement of the superstructure decreases compared with the common isolation system. Based on finite element method, the numerical models of seismic isolators with and without S-shaped steel dampers are established in ABAQUS. Meanwhile, numerical analyses under cyclic loading tests are performed. The simulation results showed that, the seismic isolator without S-shaped steel dampers usually has advantages in absorbing the energy, but the deformation is larger. S-shaped steel dampers showed more dissipative energy capacity in the novel hybrid system, which is better than the common seismic isolator. Meanwhile, steel dampers also can decrease the deformation of the seismic isolator to keep the superstructure safe. The mechanical properties of seismic isolator with and without S-shaped steel dampers are obviously different, such as dissipative energy capacity and structural period. The seismic isolator coupled with S-shaped steel dampers has better mechanical capacity to compensate the disadvantages of seismic isolator without S-shaped steel dampers. Therefore, it can be adopted as a reference to solve the problem of safety in the engineering practice.

Keywords: Seismic isolator, S-shaped steel damper, Dissipative energy capacity, Finite element method.

ISSN:2623-3347 © 2023 The Authors. Published by Eccomas Proceedia.
Peer-review under responsibility of the organizing committee of COMPDYN 2023.
doi: 10.7712/120123.10504.20305

1 INTRODUCTION

The investigation of a small historical masonry church using fiber reinforced elastomeric isolators in bonded and unbonded applications is to improve seismic performance. [1] And the fiber reinforced elastomeric isolators which are made of the recycling used rubber from tire industry or other sources are investigated and tested. [2]

In the commercial isolators, there are natural rubber (NB), high-damping rubber (HDRB), lead rubber bearing (LRB), fiber reinforced elastomeric isolator (FREI) including bonded (BFREI) and unbonded (UFREI). [2]

In the developing countries, low-cost unbonded fiber reinforced elastomeric seismic isolation systems applied in new masonry buildings are simulated and the simplified numerical model is proposed to predict the behavior of the seismic isolation system. [3] Moreover, unbonded fiber reinforced elastomeric isolator can require no expensive thick steel plates and reduce the seismic demand. [4]

In the recent years, there are the hybrid seismic isolation systems proposed which are the promising devices. The hybrid seismic base isolation of a historical masonry church using unbonded fiber reinforced elastomeric isolators and shape memory alloy wires significantly increases the energy dissipation capacity of the base isolation system and decreases the horizontal displacements of the masonry building. [5]

The new hybrid isolator consists of elastomeric bearing, sliding parts and yielding dampers (friction-yielding-elastomeric bearing (FYEB)), which absorb the energy from the friction-yielding part and support the vertical action from rubber pads. [6]

Another innovative seismic isolator device proposed is slit steel rubber bearing (SSRB) which has better energy dissipation capacity than the corresponding value of LRB and lower shear strain rather than LRB. [7]

Seismic isolator has the limitation of energy dissipation capacity and also has the large horizontal deformation. However, steel damper has advantages in dissipative energy capacity and damping ratio. In this paper, the traditional and novel hybrid seismic isolation systems including seismic isolator with and without S-shaped steel dampers (SSSDs) are simulated and investigated to supply the practical application in the field of civil engineering.

2 THEORETICAL ANALYSIS

There are two factors of seismic isolators with different rubber thicknesses, such as shape factor and aspect ratio, as followed in Table 1.

No.	Total thickness of rubber layer t_r (mm)	Total thickness of steel laminae t_s (mm)	Shape factor $S=\frac{a}{4t}$	Aspect ratio $R=\frac{a}{h}$
1	50	2	3.75	
2	48	4	3.91	2.88
3	46	6	4.08	

Table 1: Parameters of seismic isolators with different rubber thicknesses.

Based on the theory [8, 9], it is to estimate the mechanical capacities of the traditional and novel hybrid systems. There are the formulas of mechanical properties as followed in Equations (1)-(5), which can represent the main characters of seismic isolation device.

$$K_{h,eff} = \frac{\left(F_{\max} - F_{\min}\right)}{\left(\Delta_{\max} - \Delta_{\min}\right)} \tag{1}$$

$$\xi = \frac{W_d}{4\pi W_s} \tag{2}$$

$$W_s = \frac{1}{2} K_{h,eff} \Delta_{ave}^2 \tag{3}$$

$$\Delta_{ave} = \frac{1}{2}\left(\left|\Delta_{\max}\right| + \left|\Delta_{\min}\right|\right) \tag{4}$$

$$T_h = 2\pi \sqrt{\frac{pA}{gK_{h,eff}}} \tag{5}$$

$K_{h,eff}$ is effective horizontal stiffness of seismic isolation device, p and A are constant vertical pressure and plane area of seismic isolation device. $F_{\max}$ and $F_{\min}$ are the maximum and minimum horizontal forces obtained in each side of loading cycle in Equation 1, respectively. $\Delta_{\max}$ and $\Delta_{\min}$ are the maximum and minimum horizontal displacements obtained in each side of loading cycle in Equations 1 and 4, respectively. In Equation 4, Δ_{ave} is equal to the average of absolute value displacement of $\Delta_{\max}$ and $\Delta_{\min}$. W_d is the dissipated energy in each cycle which is equal to the area inside the force-displacement hysteresis curve, and W_s is stored energy in the hybrid system shown in Equation 3. T_h is horizontal period in Equation 5.

According to Equations (1)-(5), the data of seismic isolator without SSSDs are calculated in the Tables 2-4. The ideal hybrid system period (T*) is 0.8 times more than theoretical calculation. Corresponding to different rubber thicknesses and pressures, the objectives of the hybrid system period are shown in Tables 2-4.

No.	Total thickness of rubber layer t_r (mm)	Total thickness of steel laminae t_s (mm)	Pressure p (MPa)	Horizontal period T (s)	Hybrid system period T*⩾0.8T (s)
1			3	0.869	⩾0.695
2	50	2	4	1.004	⩾0.803
3			5	1.122	⩾0.898

Table 2: Theoretical calculation for seismic isolator with 50mm of total rubber thickness.

No.	Total thickness of rubber layer t_r (mm)	Total thickness of steel laminae t_s (mm)	Pressure p (MPa)	Horizontal period T (s)	Hybrid system period T*⩾0.8T (s)
1			3	0.852	⩾0.681
2	48	4	4	0.983	⩾0.787
3			5	1.099	⩾0.879

Table 3: Theoretical calculation for seismic isolator with 48mm of total rubber thickness.

No.	Total thickness of rubber layer t_r (mm)	Total thickness of steel laminae t_s (mm)	Pressure p (MPa)	Horizontal period T (s)	Hybrid system period T*≥0.8T (s)
1			3	0.834	≥0.667
2	46	6	4	0.963	≥0.770
3			5	1.076	≥0.861

Table 4: Theoretical calculation for seismic isolator with 46mm of total rubber thickness.

3 NUMERICAL ANALYSIS

3.1 Material property

In the research project, the novel hybrid seismic isolation system has two main types of materials, rubber and steel. The coefficients of the mechanical properties of standard rubber are adopted in numerical investigation in Tables 5-6. The steel material of the novel isolation device is made of common steel, which has the value of Young's modulus and the yield strength, 206 GPa and 345MPa, respectively.

Type	C_{10}	C_{20}	C_{30}	D_i
Standard rubber	0.40746	0.0019039	-0.000031585	0

Table 5: Coefficients of the Yeoh hyperelastic model for rubber.

Type	g_1	τ_1	g_2	τ_2
Standard rubber	0.132	0.0203	0.207	8.03

Table 6: Coefficients of the Prony series model for rubber.

3.2 Numerical model

The geometric properties of seismic isolator with and without SSSDs is shown in Table 7. In Figures 1 (a) and 1 (b), the model of the novel isolation device is built in ABAQUS. [10] Rubber pads are welded with steel laminas with dimensions 150×150×52mm^3.

S-shaped steel dampers of the novel hybrid seismic isolation system are bolted between upper and lower connection plates in Figure 1 (b). The surfaces of steel laminae and rubber layers are connected by tie contact. The surfaces of steel damper and connection plates are contacted by friction contacts. The friction coefficient 0.3 has been applied in the model using surface to surface contact in ABAQUS.

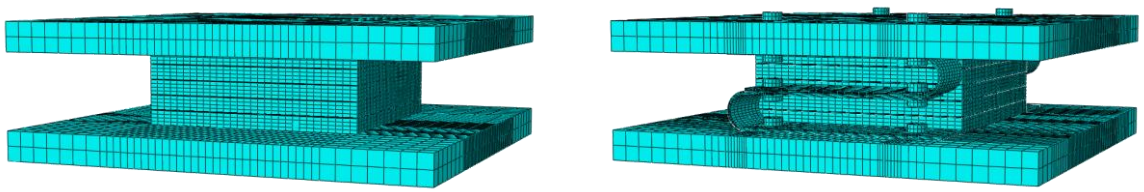

(a) (b)

Figure 1: ABAQUS models of seismic isolator without (a) and with (b) SSSDs.

The seismic isolator with and without SSSDs have been modeled using over 80000 eight node brick elements (C3D8RH for rubber and C3D8R for steel) in Figures 1 (a) and 1 (b). The mechanical properties of the numerical models have been analyzed and compared under different vertical pressures and cyclic loading tests to identify the advantages and disadvantages.

Number of rubber pad	Thickness of single rubber pad (mm)	Total thickness of rubber layer t_r (mm)	Number of steel lamina	Thickness of single steel lamina (mm)	Total thickness of steel laminae t_s (mm)	Thickness of S-shaped steel damper t_{sd} (mm)	Width of S-shaped steel damper w_{sd} (mm)
5	10	50	4	0.5	2	2	40
	9.6	48		1.0	4		
	9.2	46		1.5	6		

Table 7: Geometric properties of seismic isolator with and without SSSDs.

3.3 Simulation work

The seismic isolator with and without SSSDs in Tables 8-13 have been subjected to a 0.5 Hz cyclic horizontal displacement up to 100% Δ (50mm, 48mm, 46mm) which is the total thickness of the rubber layers applied on the top connection plate, under different vertical pressure of 3 N/mm^2, 4 N/mm^2 and 5 N/mm^2. Meantime, the lower connection plate is bolted to the fixed supports. The numerical results of seismic isolator with and without SSSDs are shown in Figures 2-19 and compared with the results to identify the differences of seismic isolator with and without SSSDs.

- The data of seismic isolator with and without SSSDs have shown in Table 8-9 at 50mm of cyclic loading tests and different vertical pressures.

No.	Total thickness of rubber layer t_r (mm)	Total thickness of steel laminae t_s (mm)	Pressure p (MPa)	Effective horizontal stiffness K_h (N/mm)	Horizontal period T' (s)
1	50	2	3	296.949	0.957
2			4	285.620	1.127
3			5	273.519	1.287

Table 8: Parameters of seismic isolator without SSSDs at 50mm of cyclic loading tests.

No.	Total thickness of rubber layer t_r (mm)	Total thickness of steel laminae t_s (mm)	Pressure p (MPa)	Effective horizontal stiffness $K_{h,eff}$ (N/mm)	Horizontal period T'' (s)
1	50	2	3	365.776	0.862
2			4	348.469	1.020
3			5	345.785	1.145

Table 9: Parameters of seismic isolator with SSSDs at 50mm of cyclic loading tests.

- In Figures 2-7, the numerical results of the models loading under 100% Δ (50mm) of cyclic loading tests and different vertical pressures represent force-displacement curves and Mises stress contour plots.

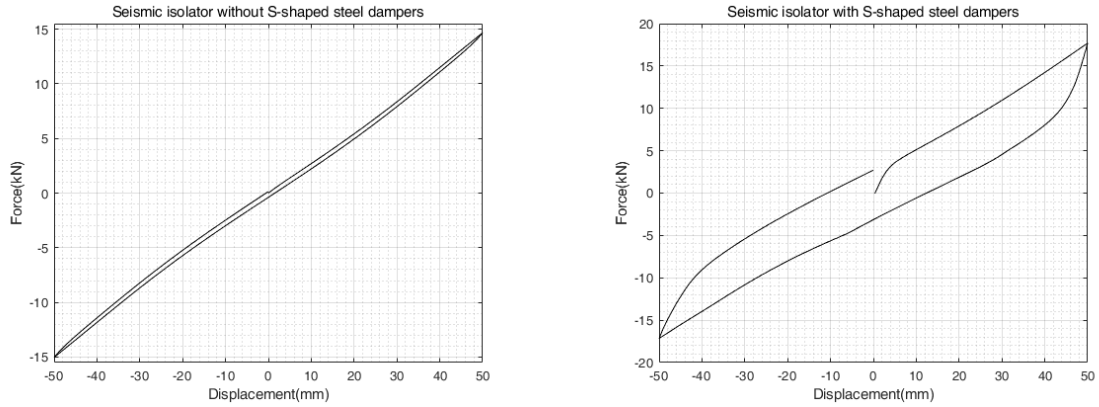

(a) (b)

Figure 2: Force – displacement curves of seismic isolator without (a) and with (b) SSSDs under 3 MPa of pressure.

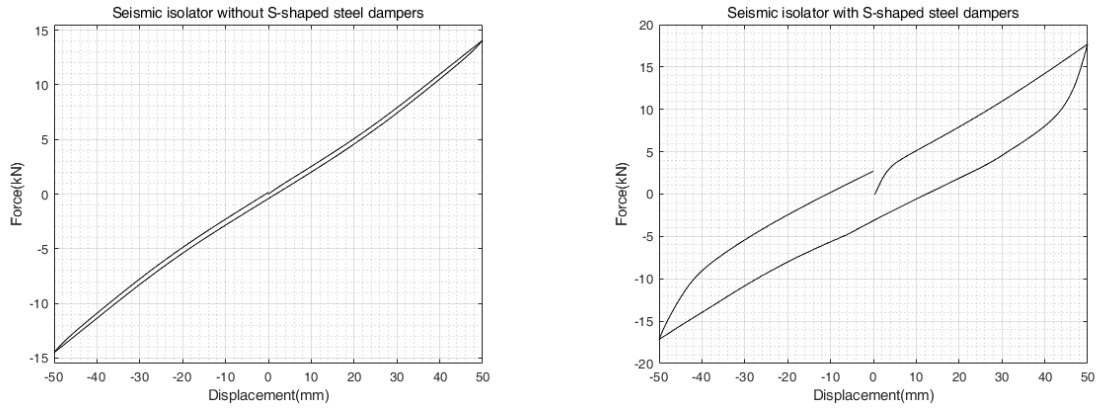

(a) (b)

Figure 3: Force – displacement curves of seismic isolator without (a) and with (b) SSSDs under 4 MPa of pressure.

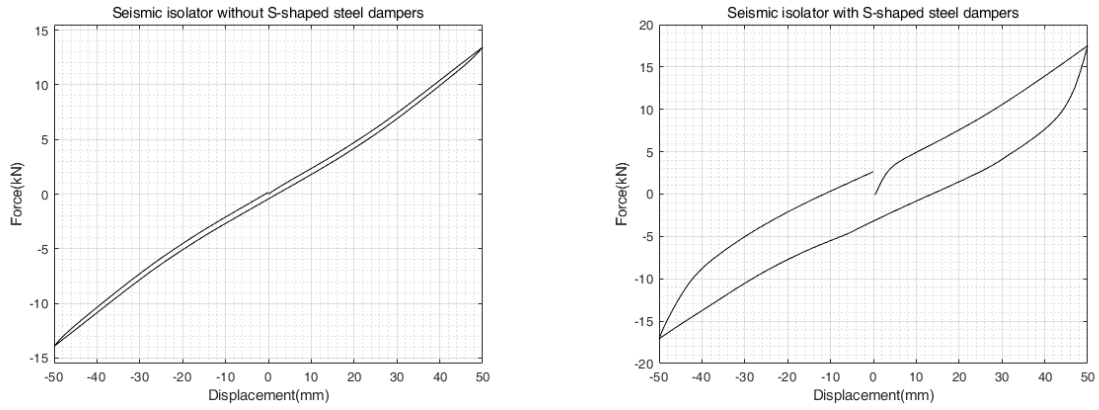

(a) (b)

Figure 4: Force – displacement curves of seismic isolator without (a) and with (b) SSSDs under 5 MPa of pressure.

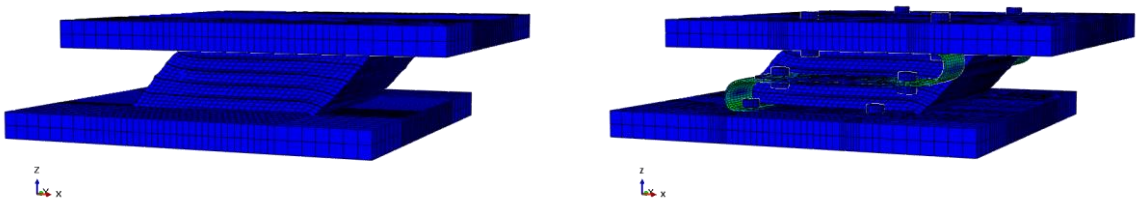

(a) (b)

Figure 5: Numerical comparisons of seismic isolator without (a) and with (b) SSSDs under 3 MPa of pressure.

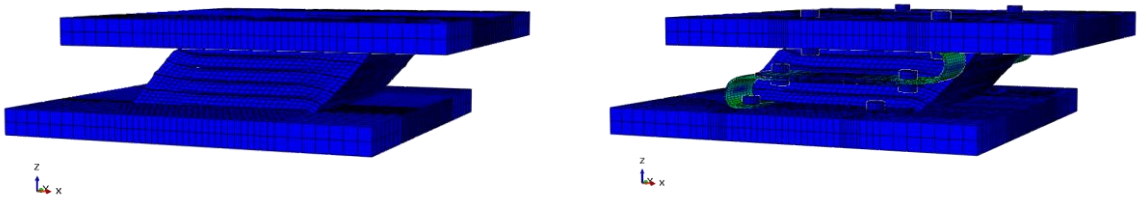

(a) (b)

Figure 6: Numerical comparisons of seismic isolator without (a) and with (b) SSSDs under 4 MPa of pressure.

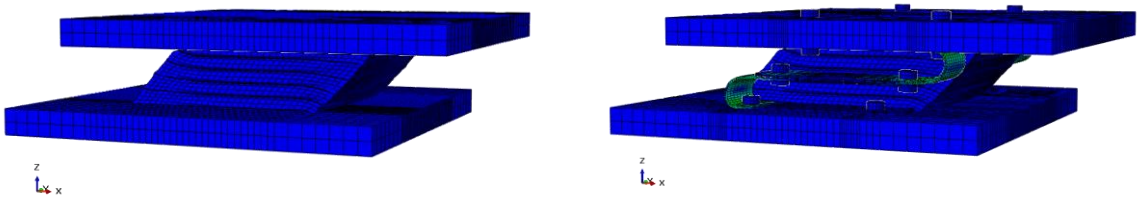

(a) (b)

Figure 7: Numerical comparisons of seismic isolator without (a) and with (b) SSSDs under 5 MPa of pressure.

- The data of seismic isolator with and without SSSDs have shown in Tables 10-11 at 48mm of cyclic loading tests and different vertical pressures.

No.	Total thickness of rubber layer t_r (mm)	Total thickness of steel laminae t_s (mm)	Pressure p (MPa)	Effective horizontal stiffness K_h (N/mm)	Horizontal period T' (s)
1			3	311.912	0.934
2	48	4	4	301.324	1.097
3			5	290.016	1.250

Table 10: Parameters of seismic isolator without SSSDs at 48mm of cyclic loading tests.

No.	Total thickness of rubber layer t_r (mm)	Total thickness of steel laminae t_s (mm)	Pressure p (MPa)	Effective horizontal stiffness $K_{h,eff}$ (N/mm)	Horizontal period T'' (s)
1			3	380.754	0.845
2	48	4	4	365.710	0.996
3			5	364.271	1.115

Table 11: Parameters of seismic isolator with SSSDs at 48mm of cyclic loading tests.

- In Figures 8-13, the numerical results of the models loading under 100% Δ (48mm) of cyclic loading tests and different vertical pressures represent force-displacement curves and Mises stress contour plots.

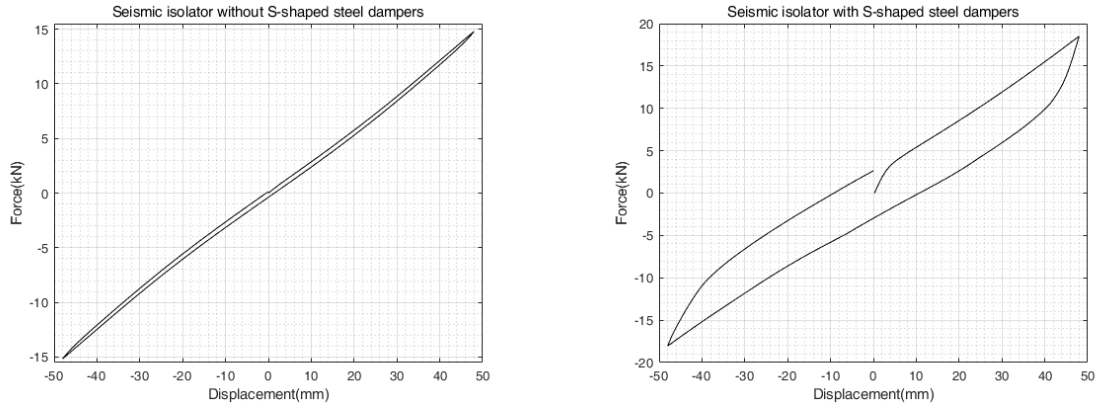

(a) (b)

Figure 8: Force – displacement curves of seismic isolator without (a) and with (b) SSSDs under 3 MPa of pressure.

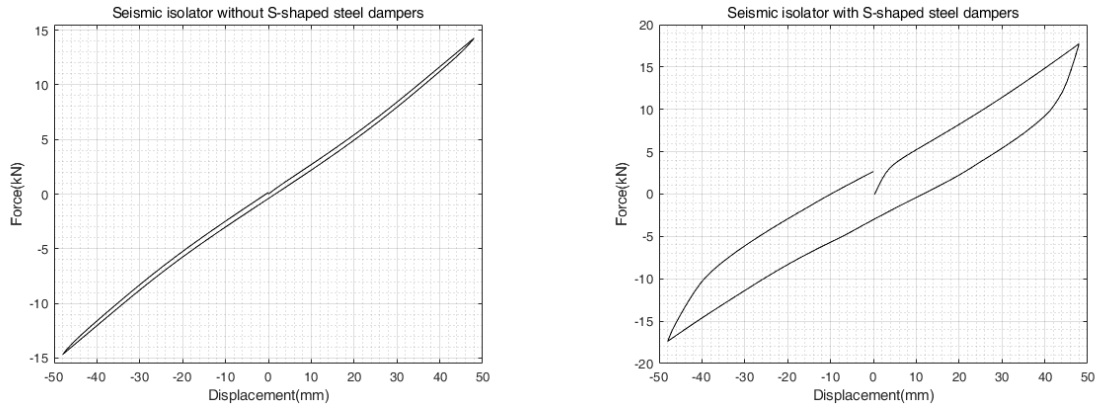

(a) (b)

Figure 9: Force – displacement curves of seismic isolator without (a) and with (b) SSSDs under 4 MPa of pressure.

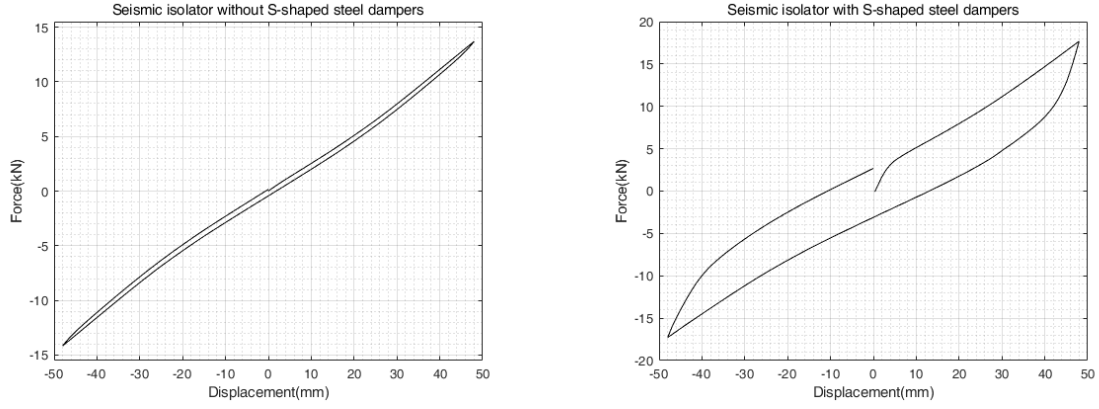

(a) (b)

Figure 10: Force – displacement curves of seismic isolator without (a) and with (b) SSSDs under 5 MPa of pressure.

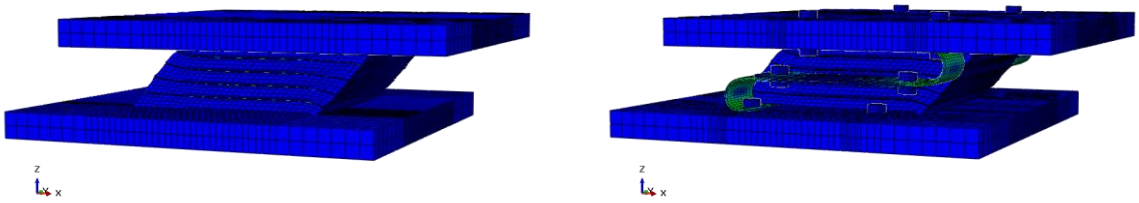

(a) (b)

Figure 11: Numerical comparisons of seismic isolator without (a) and with (b) SSSDs under 3 MPa of pressure.

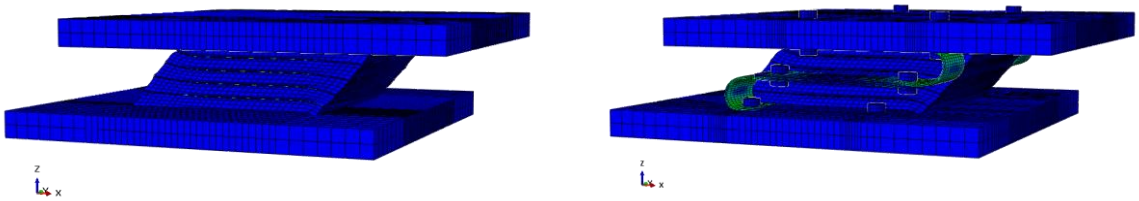

(a) (b)

Figure 12: Numerical comparisons of seismic isolator without (a) and with (b) SSSDs under 4 MPa of pressure.

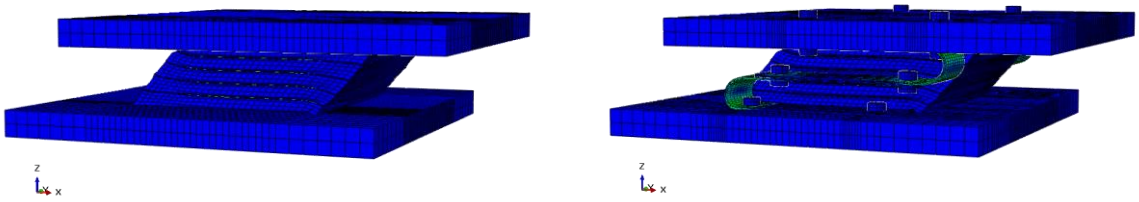

(a) (b)

Figure 13: Numerical comparisons of seismic isolator without (a) and with (b) SSSDs under 5 MPa of pressure.

- The data of seismic isolator with and without SSSDs have shown in Tables 12-13 at 46mm of cyclic loading tests and different vertical pressures.

No.	Total thickness of rubber layer t_r (mm)	Total thickness of steel laminae t_s (mm)	Pressure p (MPa)	Effective horizontal stiffness K_h (N/mm)	Horizontal period T' (s)
1			3	327.921	0.911
2	46	6	4	318.031	1.068
3			5	307.481	1.214

Table 12: Parameters of seismic isolator without SSSDs at 46mm of cyclic loading tests.

No.	Total thickness of rubber layer t_r (mm)	Total thickness of steel laminae t_s (mm)	Pressure p (MPa)	Effective horizontal stiffness $K_{h,eff}$ (N/mm)	Horizontal period T'' (s)
1			3	399.357	0.825
2	46	6	4	386.760	0.968
3			5	383.353	1.087

Table 13: Parameters of seismic isolator with SSSDs at 46mm of cyclic loading tests.

- In Figures 14-19, the numerical results of the models loading under 100% Δ (46mm) of cyclic loading tests and different vertical pressures represent force-displacement curves and Mises stress contour plots.

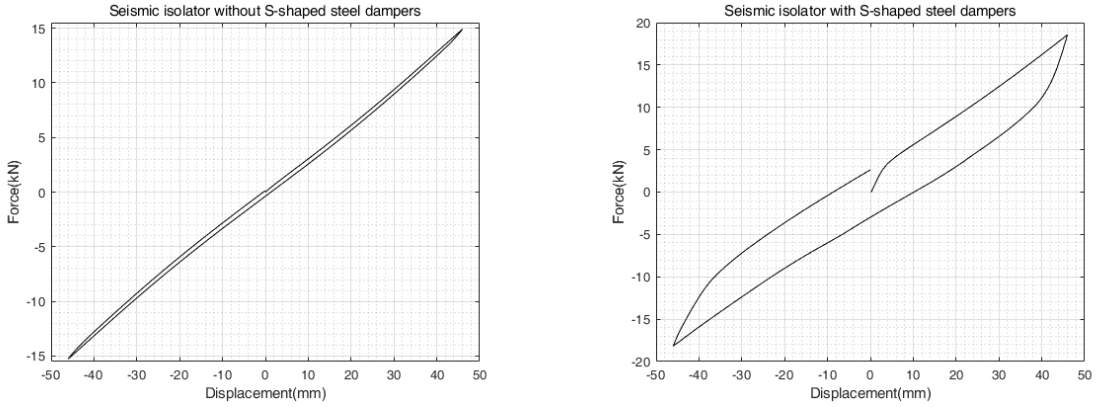

(a) (b)

Figure 14: Force – displacement curves of seismic isolator without (a) and with (b) SSSDs under 3 MPa of pressure.

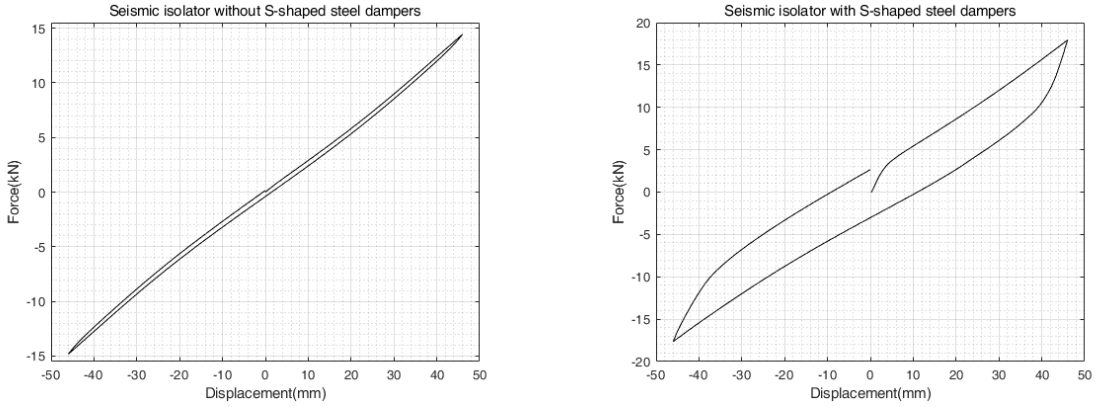

(a) (b)

Figure 15: Force – displacement curves of seismic isolator without (a) and with (b) SSSDs under 4 MPa of pressure.

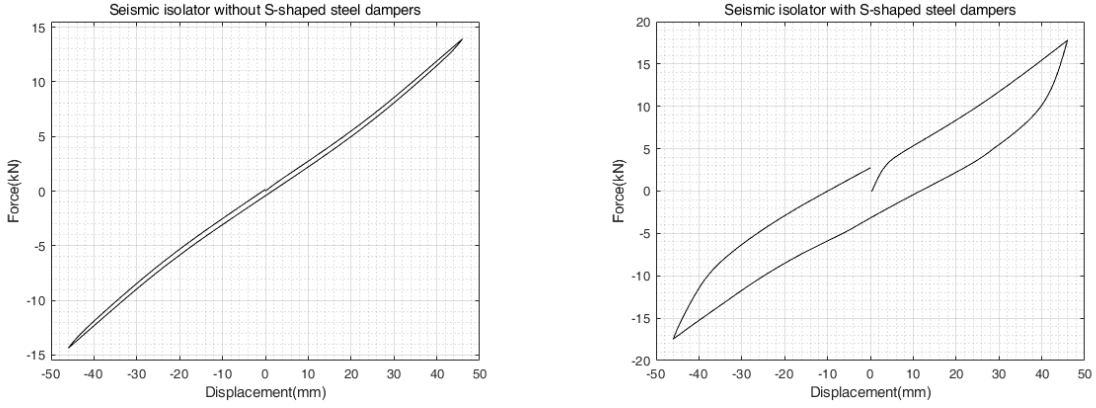

(a) (b)

Figure 16: Force – displacement curves of seismic isolator without (a) and with (b) SSSDs under 5 MPa of pressure.

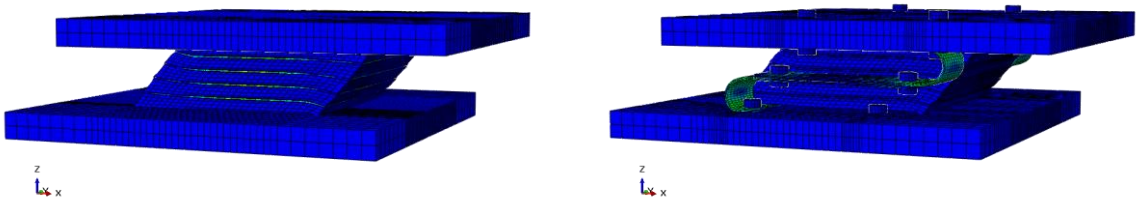

(a) (b)

Figure 17: Numerical comparisons of seismic isolator without (a) and with (b) SSSDs under 3 MPa of pressure.

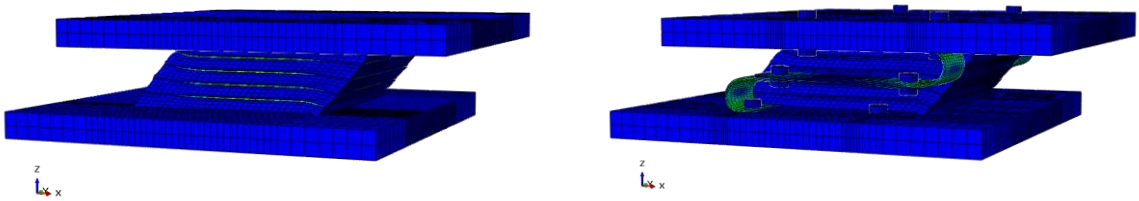

(a) (b)

Figure 18: Numerical comparisons of seismic isolator without (a) and with (b) SSSDs under 4 MPa of pressure.

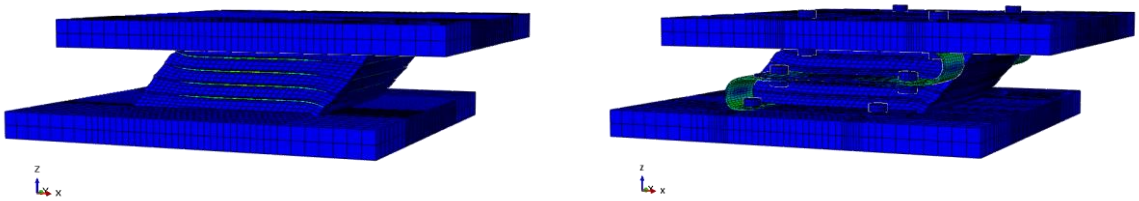

(a) (b)

Figure 19: Numerical comparisons of seismic isolator without (a) and with (b) SSSDs under 5 MPa of pressure.

3.4 Comparison analysis

By ABAQUS software [10], it is investigated the mechanical property of seismic isolator coupled with S-shaped steel dampers. The FE models of seismic isolator with SSSDs in ABAQUS are built and compared with seismic isolator without SSSDs.

In the same condition of shape factor and aspect ratio, seismic isolator with and without SSSDs under higher vertical pressure have lower effective horizontal stiffness. Under the same vertical pressure, seismic isolator with and without SSSDs including higher shape factor have higher effective horizontal stiffness.

According to the theoretical calculations in Tables 8-13, the promising objectives of the hybrid system period ($\geqslant$0.8T) in Tables 2-4 are achieved. Comparing with the seismic isolator without SSSDs, the effective horizontal stiffness of seismic isolator with SSSDs obviously increases 20% more than that of seismic isolator without SSSDs.

In the cyclic loading tests, the area of the force-displacement curves of seismic isolator with SSSDs under different horizontal displacements and pressures are evidently much bigger than seismic isolator without SSSDs in Figures 2-19, which means that seismic isolator with

SSSDs has more dissipative energy ability from S-shaped steel dampers rather than seismic isolator without SSSDs. Steel dampers of the novel hybrid system can dissipate more energy under the same displacement of cyclic loading comparing with seismic isolator without SSSDs. By adding S-shaped steel dampers the novel hybrid system has advantages in the aspect of energy dissipation capacity.

4 CONCLUSIONS

In this research, 3D finite element models of seismic isolator coupled with and without SSSDs have been established and analyzed under different pressures (3MPa, 4MPa, 5MPa) and cyclic loads (50mm, 48mm, 46mm) to study the performance, and have been compared with them to identify the advantages and disadvantages.

The seismic isolator with and without SSSDs have the same influence under different shape factors and vertical pressures. With lower shape factor and higher vertical pressure, the novel hybrid system period is longer.

The period of the novel hybrid system is more than the objective period of the hybrid system in Tables 2-4, which is a promising hybrid system in the practical project. Meanwhile, the effective horizontal stiffness of seismic isolator with SSSDs increases 20% more than seismic isolator without SSSDs in Tables 8-13.

Compared with seismic isolator without SSSDs, it is obviously to improve the mechanical property of the hybrid system under different pressures and cyclic loading tests because of the advantages of S-shaped steel dampers. The novel hybrid system has more advantages in the aspect of energy dissipation capacity than seismic isolator without SSSDs. According to the area of force-displacement, seismic isolator by adding S-shaped steel dampers evidently increases. The novel hybrid system has more dissipative energy capacity when S-shaped steel dampers work effectively. Therefore, it can be adopted to supply the practical application in the field of civil engineering.

ACKNOWLEDGEMENTS

The author Kai Guo who is studying in Politecnico di Milano, Italy would like to acknowledge the financial support received by the China Scholarship Council (CSC) for the PhD program.

REFERENCES

[1] A.B. Habieb, M. Valente, G. Milani, Base seismic isolation of a historical masonry church using fiber reinforced elastomeric isolators. *Soil Dynamics and Earthquake Engineer*, 120, 127-145, 2019.

[2] A.B. Habieb, G. Milani, R. Cerchiaro, et al, Numerical study on rubber compounds made of reactivated ethylene propylene diene monomer for fiber reinforced elastomeric isolators. *Polymer Engineering Science*, 61, (1), 258-277, 2021.

[3] A.B. Habieb, G. Milani, T. Tavio, Two-step advanced numerical approach for the design of low-cost unbonded fiber reinforced elastomeric seismic isolation systems in new masonry buildings. *Engineering Failure Analysis*, 90, 380–96, 2018.

[4] A.B. Habieb, M. Valente, G. Milani, Implementation of a simple novel Abaqus user element to predict the behavior of unbonded fiber reinforced elastomeric isolators in macro-scale computations. *Bulletin of Earthquake Engineering*, 17, (5), 2741–2766, 2019.

[5] A.B. Habieb, M. Valente, G. Milani, Hybrid seismic base isolation of a historical masonry church using unbonded fiber reinforced elastomeric isolators and shape memory alloy wires. *Engineering Structures*, 196, 109281, 2019.

[6] A.H. Haeri, K. Badamchi, H.T. Riahi, Proposing a new hybrid friction yielding elastomeric bearing. *Journal of Vibration and Control*, 25, (9), 1558-1571, 2019.

[7] M. Saadatnia, H.T. Riahi, M. Izadinia, The effect of cyclic loading on the rubber bearing with slit damper devices based on finite element method. *Earthquakes and Structures*, 18, (2), 215-222, 2020.

[8] J.M. Kelly, The current status of seismic isolation technology in the United States. *International Atomic Energy Agency (IAEA)*, 87, 89-111, 1992.

[9] H.C. Tsai, J.M. Kelly, Stiffness analysis of fiber-reinforced rectangular seismic isolators. *Journal of Engineering Mechanics*, 128, (4), 462–70, 2002.

[10] Abaqus/Standard User's Manual, Version 6.14.